Since January 2020 Elsevier has created a COVID-19 resource centre with free information in English and Mandarin on the novel coronavirus COVID-19. The COVID-19 resource centre is hosted on Elsevier Connect, the company's public news and information website.

Journal of Infection and Public Health 14 (2021) 324–330

Contents lists available at ScienceDirect

Journal of Infection and Public Health

journal homepage: http://www.elsevier.com/locate/jiph

Synthesis of silver nanoparticles using gum Arabic: Evaluation of its inhibitory action on *Streptococcus mutans* causing dental caries and endocarditis

Mysoon M. Al-Ansari [a,*], Nora D. Al-Dahmash [a], A.J.A. Ranjitsingh [b]

[a] *Department of Botany and Microbiology, College of Science, King Saud University, Riyadh, 11451, Saudi Arabia*
[b] *Department of Biotechnology, Prathyusha Engineering College, Chennai 600056, India*

ARTICLE INFO

Article history:
Received 3 November 2020
Received in revised form
14 December 2020
Accepted 19 December 2020

Keywords:
S. mutans
Gum Arabic
Acacia senegal
NPs
Oral hygiene

ABSTRACT

Background: Streptococcus mutans are an oral pathogen that causes dental caries, endocarditis, and systemic dysfunctions, an alternative antibacterial solution from silver nanoparticles (AgNPs) are investigated.

Methods: AgNPs were synthesized using the ethnobotanical product gum Arabic. It influenced the nanoparticles with medicinal value through their role as capping, stabilizing, or surface-attached components. The biophysical characteristics of the synthesized AgNPs were studied using UV–vis spectrum, XRD, EDAX, SEM, and TEM tools. The AgNPs were spherical with the average size less than 10 nm. By using the well diffusion and microdilution techniques, the impact of synthesized AgNPs was tested against *S. mutans* isolates.

Results: The smaller the size, the greater the antibacterial and antiviral potential the particles exhibit. The biophysical characteristics of AgNPs the presence of phenols, alcohols, amides, sulfoxide, flavanoids, terpenoids and steroids. The AgNPs exhibited a good antibacterial action against the oral pathogen *S. mutans*. The synthesized NPs at a dose level of 200 μg/mL exhibited an inhibition zone with 18.30 ± 0.5 nm diameter. The synthesised nanoparticles inhibited the genes responsible for biofilm formation of *S. mutans* over host tooth and gums (gtfB, gtfc, gtfD) and virulent protective factors (comDE, brpA and smu 360) and survival promoter genes (gyrA and spaP, gbpB).

Conclusion: The potent antibiotic action over *S. mutans* seen with the synthesized NPs, paves the way for the development of novel dental care products. Also, the small-sized NPs promote its applicability in COVID-19 pandemic containment.

Introduction

The emerging drug resistance microbes, evolving new type of infections, untimely availability of prophylactic vaccines against pandemic viral infections necessitates the need to get solutions from alternative medicines. In this quest to find alternative medicine for SARS-CoV-2 and other oral hygiene problems, attention is focused on pharmaceutical nanotechnology [1]. Nanoparticles synthesized using bio products are a possible remedy for COVID-19 after a proper clinical evaluation [2,3]. The practical trials at the home level or endemic population level or at the animal model level, the silver nanoparticles stand right for treating dental caries caused by *Streptococcus mutans* and respiratory infections caused by coronaviruses.

It is reported that the silver nanoparticles prevent the formation of *S. mutans* biofilm over teeth and inhibit the quorum sensing to prevent dental caries [4,5]. The AgNPs are reported to stand against COVID-19 as a disinfectant, diagnostic tools, drug-delivering vehicle, and suppress immune response to COVID-19 [1,2,6–8]. According to Oron Zachar, colloidal nanoparticles in the size range 3–7 nm can effectively block SARS-CoV-2 viral attachment with the host's cell [9]. AgNPs can be used with bronchodilators through nebulization to get relief from COVID-19 [10]. There are several reports on the biomedical importance of AgNPs synthesized using botanicals [11,12].

As AgNPs have several biomedical and other applications, attention being carried out to synthesis the AgNPs using biogenic agents and its application as antimicrobial antioxidant, anticancer, antivi-

* Corresponding author.
E-mail address: myalansari@ksu.edu.sa (M.M. Al-Ansari).

https://doi.org/10.1016/j.jiph.2020.12.016

ral, and pharmaceutical agents for many ailments [13,14]. In the current approach, a novel method of using tree exudates with a high amount of polysaccharides in gum Arabic [GA] derived from the tree, *Acacia senegal* (L) Wild, was used to synthesize AgNPs. This resin is a polymer with glycoproteins and polysaccharides. Arabinose and galactose present in the gum give a good binding capacity and are used in the food industry [15]. This water-soluble, edible glue is used in food, pharmaceutical, and industrial applications. Why the gum Arabic is used as a moderating agent to prepare AgNPs is because GA exerts its components over NPs as capping agents change Zeta potential to negative and causes aggregation process [16]. Using GA as a growth medium for nickel nanoparticle preparation enhances excellent antibacterial behaviour [17]. Further GA exuded from *A. senegal* was proved to be an immunomodulatory agent in COVID-19 patients [18]. Using the natural polymers of GA as a stabilizer promoted capping in nanoparticles and enhanced the compatibility of AgNPs for pharmaceutical and biomedical applications [19]. As the natural polymers in the GA can tune up the synthesis nanoparticles with biomedical potential, in the present study it is planned to synthesize AgNPs using GA. In the present study, the synthesized AgNPs are tested against *S. mutans* that cause biofilm and induce dental caries. Dental caries is a significant problem among the citizens of Saudi Arabia. In Saudi Arabia, dental caries was reported in 85.77% of children in the age group 6 years and 71.35% in the 15 years group [20].

Materials and methods

Bacterial strains and culture medium

The oral pathogen *S. mutans* ATCC 25175 was obtained from Dentistry College at King Khalid Hospital. The strain was grown on Nutrient Agar media (NA) at 37 °C for 24 hand used for further study. All the media components and analytical reagents were purchased from, Sigma Aldrich Chemicals, USA, and Watin-Biolife Advanced diagnostics manufacturing Co., Saudi Arabia.

Preparation of gum Arabica extracts and AgNPs synthesis

The bio-reduction agent chosen to synthesis of AgNPs is the glue called gum Arabic [GA]. The gum granules were procured from a supplier from Riyadh, Saudi Arabia. Five gram GA powder was dissolved in a specific volume (100 mL) of deionized water and filtered with a filter paper. 50 mL of acacia aqueous extract added to 3 mM of $AgNO_3$ with in a 250 mL of distilled water. In the bio-reduction process the colorless solution developed dark yellow color. The change in color indicated the synthesis of GA-AgNPs**.** The synthesized AgNPs were collected by centrifugation (15,000 rpm, 25 min) and purified by washing three times with sterile double distilled water and finally air-dried. The air-dried GA-AgNPs were lyophilized in ambient conditions, and it was stored in a screw cap bottle for further characterization and antibacterial activity studies.

Bio-physical characterization of GA-AgNPs

The formation of GA-AgNPs was tested by the characteristic surface Plasmon resonance (SPR) peak through a UV–vis spectrophotometer (Shimadzu, UV-240, HitachiU-3200). The XRD spectra were recorded and analyzed for the bio-synthesized GA-AgNPs with PANalytical X'Pert PRO X-ray diffractometer. The size and morphology of GA-AgNPs were examined by using the Transmission electron microscopy-[HR-TEM model on a JEOL JEM 2100]. Scanning electron microscopy was done by using (SEM) Jeol7610. The elemental analysis was carried out using an Energy Dispersive X-ray analyzer. The FT-IR measurements were made using Shimadzu FTIR-8201PC instrument.

Table 1
Primers used for gene study in *S. mutans* exposed to GA-AgNPs.

Gene	FW	RV
brpA	*GGAGGAGCTGCATCAGGATTC*	*AACTCCAGCACATCCAGCAAG*
spaP	*GACTTTGGTAATGGTTATGCATCAA*	*TTTGTATCAGCCGGATCAAGTG*
Smu630	*GTTAGTTCTGGTTTTGACCGCAAT*	*CCCTCAACAACAACATCAAAGGT*
comDE	*ACAATCCTTGAGTTCCATCCAAG*	*TGGTCTGCTGCCTGTTGC*
gtfB	*CATACAGTAACGACAATCAGTAGCTCTA*	*GTACGAACTTTGCCGTTATTGTCATA*
gtfC	*GGTTTAACGTCAAAATTAGCTGTATTAGC*	*CTCAACCAACCGCCACTGTT*
gtfD	*CACAGGCAAAAGCTGAATTAACA*	*GAATGGCCGCTAAGTCAACAG*
gbpB	*ATGGCGGTTATGGACACGTT*	*TTTGGCCACCTTGAACACCT*
GyrA	*TTCGTACAAGTGTTGCCGATATCT*	*TCTAGGCGCATCACTTTGACA*

Minimum inhibitory concentration (MIC) of GA-AgNPs

The MIC value of GA-AgNPs was measured using MH broth microdilution method. Serial two-fold dilution of GA-AgNPs was prepared with the concentration ranging from 0.25 μg/mL to 2.0 μg/mL. The *S. mutans* concentration was adjusted to 10^8/CFU/mL, 0.5 Mc Farland standard. The *S. mutans* was loaded with MH broth tubes with different doses of GA-AgNPs. The control with only the broth and experimental tubes with varying doses of GA-AgNPs were incubated for 24 h at 37 °C. The MIC was the lowest concentration of GA-AgNPs where no visible growth is seen in the tubes. The control and experimental tubes' turbidity was recorded before and after the experiments to confirm MIC values.

Antibacterial study of GA-AgNPs

The inhibitory effect of GA-AgNPs on *S. mutans* was determined by the agar diffusion method. *S. mutans (*ATTC ATCC 25175) obtained were cultured in LB broth overnight. The culture's turbidity was made to 5×10^5 CFU/mL. The *S. mutans* were plated on LB agar medium (Sigma – chemicals). In the plates, 5 mm wells were made using a sterile cork borer. The diameter of the wells was 5 mm. In to each well 0.1 mL of the following concentrations of GA-AgNPs viz., 25 μg/mL, 50 μg/mL, 100 μg/mL, and 200 μg/mL were loaded and incubated at 37 °C for 24 h. After incubation, the diameter of the zones of inhibition for each concentration was recorded. A middle well was used as negative control and filled with 0.1% DMSO.

RNA isolation and RT-PCR (qRT-PCR) study

To analyze the effect of GA-AgNPs on gene expressions, *S. mutans* was cultured in Brain Heart Infusion Broth [BHI] provided by supplemented with sub MIC concentration of the extracts [5.0 μg/mL–20 μg/mL]. Overnight culture of *S. mutans* (ATCC 25175-oral pathogens) was grown in BHI medium. Bacterial culture (OD 600 = 0.8) was diluted at a ratio of 1:50 followed by their inoculation into BHI media and was incubated at 37 °C for 24 h growth. The concentration of the culture used was 0.5×105 CFU/mL. For RNA isolation, the harvested cultures were centrifuged at 4800 g for 10 min. RNA was isolated and purified using the R Neasy Mini. Kit. The cDNA was made using (Clontech Laboratories-Advantage RT-for-PCR kit protocol). ROCHE Light Cycler 96 Real-Time PCR was performed using the protocol described Li et al. [21]. The primer sequences used are shown in Table 1.

Statistical analysis

The mean and standard error of mean calculated for the results with significance $p < 0.05$.

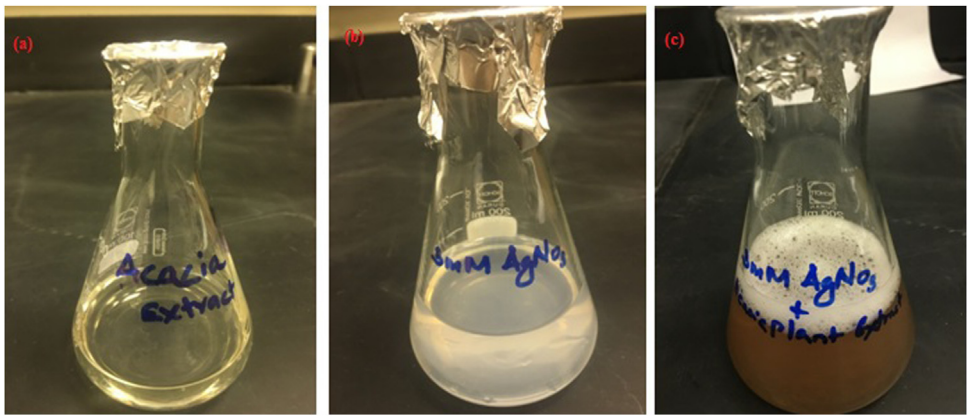

Fig. 1. Green synthesis of AgNPs formation from mixture of gum Arabic extract and silver nitrate (a). Aqueous extract of gum Arabic extract; (b). 3 mM aqueous solution of $AgNO_3$; (c). AgNPs formation.

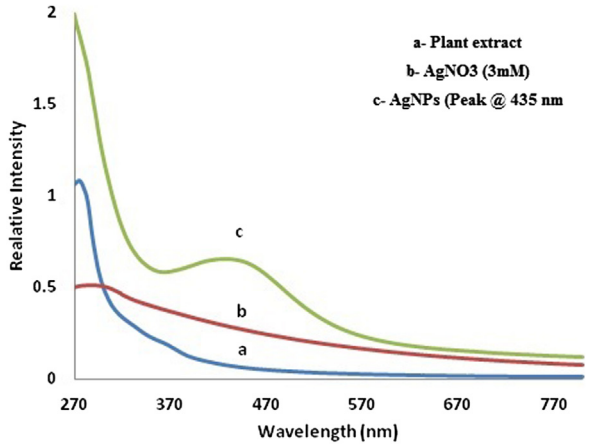

Fig. 2. Confirmative analysis of UV–vis spectrum is formation of nanoparticles. (a) Spectrum of gum Arabic extract; (b). spectrum of $AgNO_3$; (c). spectrum of AgNPs.

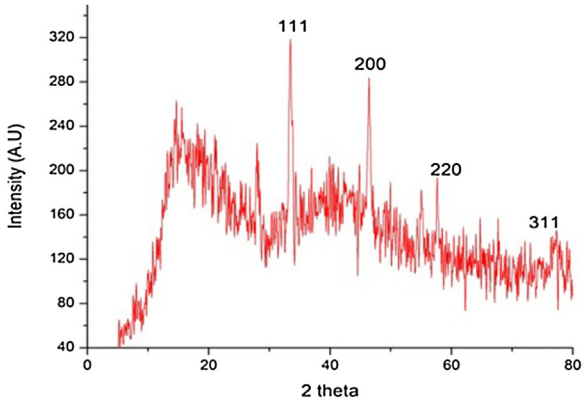

Fig. 3. Identifications of functional groups from gum Arabic powder (a) and GA-AgNPs using by FTIR.

Results and discussion

The conversion process of $AgNO_3$ to AgNPs performance was recorded by visual observation shows in Fig. 1(a–c). Fig. 1a shows fresh gum Arabic solution; Fig. 1-b combination mixture of GA solution and 3 mM of $AgNO_3$ and Fig. 1c was observed the interaction between aqueous extract of GA and $AgNO_3$. The resulting changes in the color were recorded. The change in color from light yellow to dark yellow indicated the synthesis of GA-Ag NPs.

UV–vis spectroscopy is an important technique to confirm the formation of nanoparticles. Fig. 2(a–c) illustrates the UV–vis spectra of GA extract, $AgNO_3$ and GA-AgNPs. The formation of Ag NPs was noted in the color change of reaction mixture from light yellow to dark yellow within an hour indicated the synthesis of GA-AgNPs and the Surface Plasmon Resonance (SPR) absorption band was at 420 nm. These results agreed with that reported for silver nitrate solution reduction to silver nanoparticles [11–15].

The biomolecules present in the bio tuner, GA for the formation, for the capping and stabilization of the Ag NPs were determined using FTIR studies. The functional groups present in the gum Arabica and gum Arabica mediated AgNPs were reflected in the IR spectrum wavelength with different bandwidths. The band intensities in the different positions of IR spectrum (Fig. 3a) for crude GA and GA moderated AgNPs (Fig. 3b) showed in closely related wavelengths indicating similar biomolecules and are derived from GA associating and stabilizing agents. The GA showed different prominent peaks at the wavelength position at 3422.74, 2909.71, 1624.11, 1407.11, and 1059.26 cm^{-1}. The FTIR spectrum for GA-AgNPs showed peak positions at 3399.82, 2918.39, 1648.22, 1382.94, 1234.52 and 1072.52 cm^{-1}. In the GA-AgNPs spectrum, a new peak at 1234.52 cm^{-1} was noted, which is not seen in GA-FTIR. The broad peak position at wavelength 3422.79 cm^{-1} for GA and little reduced peak at 3394.82 cm^{-1} for GA-AgNPs indicated the functional groups' alcohols and phenols with O—H stretch H-bonds. The absorption spectra observed at 2909.71 cm^{-1} for GA and 2918.39 cm^{-1} for GA-Ag NPs indicates alkanes' presence with medium C—H bond stretch. The sharp spectral peak at 1624.11 cm^{-1} for GA and little blind peak at 1648.22 cm^{-1} for GA-Ag NPs indicated the presence of strong C = stretch to alkenes.

The peak of the spectrum at the wavelength between 1410–1380 cm^{-1} indicates strong S=O stretching for sulfonyl chloride. In the FTIR spectrum of GA and GA-AgNPs, a peak wavelength with the range of 1383.94–1407.11 cm^{-1} was observed. The spectral wavelength between 1390–1310 cm^{-1} indicates a strong C—O stretching with the compound alkyl aryl ether. Also, the wavelength between 1250–1020 cm^{-1} represents medium-strength C—N stretching, indicating amine compounds' presence.

In both GA and GA-AgNPs spectrum, another peak was observed at 1059.26 cm^{-1} and 1072.52 cm^{-1}, respectively. The wavelength between 1085–1050 indicates strong C—O stretching for primary alcohol, and a peak between 1070—1030 suggests strong S=O stretching for sulfoxide. The marginal shifts are seen between the peak value of IR spectra for GA and GA-AgNPs indicates that the gum Arabica has shared its functional molecules with AgNPs in various capacities like capping spot, surface-attached and stabilizing agents. The presence of phenols, alcohols, amides, sulfoxide, fla-

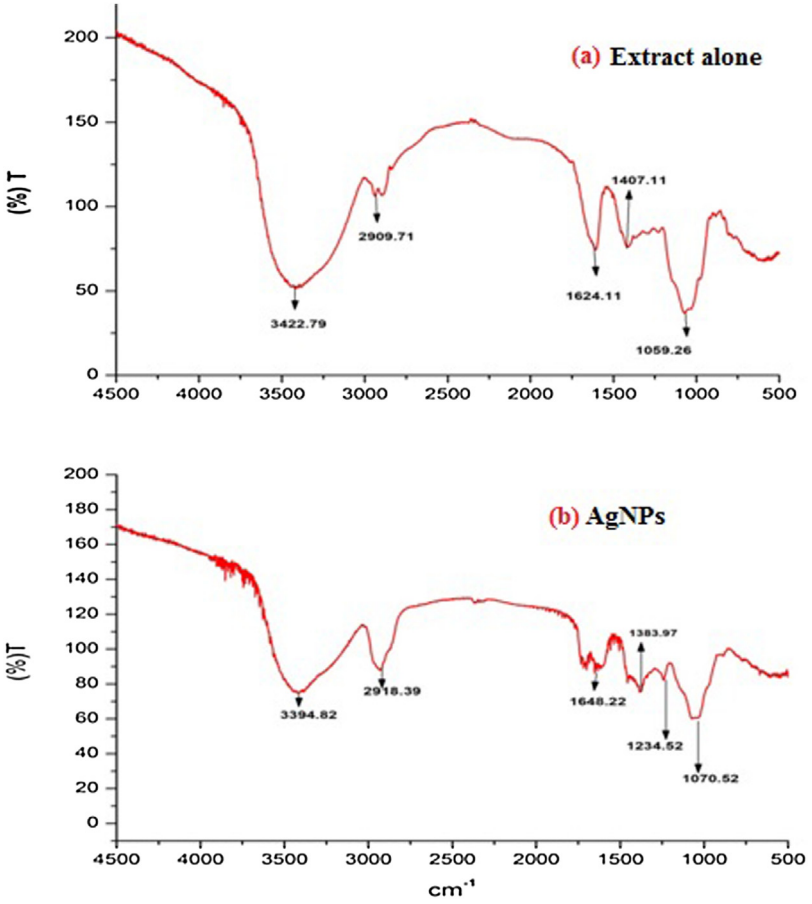

Fig. 4. The XRD- of synthesized GA-AgNPs with 2θ values.

vanoids, terpenoids and steroids etc. found in GA-AgNPs are also reported by other researchers [11–16].

X-ray diffractogram is one of the bio-physical tools to evaluate the nature of synthesized nanoparticles. The XRD-study of GA-AgNPs showed four Bragg's reflections with 2θ values of 37.21°; 48.53°; 59.23° and 77.5° corresponding to the planes (111), (200), (220) and (311) respectively. In addition to these peaks several weak peaks were noticed (Fig. 4). The prominent sharp peaks, on correlation with the reference (JCPDS) card, no.04-indicated the crystalline nature of GA-AgNPs with a face-centred cubic (fcc) structure as reported by earlier workers.

$$D = 0.9\lambda/B\cos\theta T = 0.9\lambda/B\cos\theta$$

Using the Debye–Scherrer Eq. The average size of NPs, width of Bragg's reflection at 111, and the corresponding average size of the GA-AgNPs, was found to be 11.0 nm. The presence of several unassigned peaks indicates that the GA-AgNPs have bio-organic compounds derived from gum Arabic on their surfaces, as reported by several other workers [11–16].

The SEM image of GA-AgNPs (Fig. 5-a) shows a dense population of nanoparticles with oval, spherical, and nearly spherical shapes. The EDAX spectrum of synthesizing GA-AgNPs (Fig. 5b) indicates silver with a strong signal peak at 3KeV, as reported by previous workers [22].

Transmission electron microscopic study on the biogenic GA-AgNPs (Fig. 5c), shows the presence of spherical and oval or quasi-spherical shaped nanoparticles in the size range 3.672–13.672 nm diameter with an average of 8.41 nm among 100 NPs observed using 80,000× magnification. The NPs are dispersed uniformly without any suggestion except few couplets. The TEM image at the magnification 60,000× (Fig. 5d) showed the nanoparticles in the size range 9.636 nm–36.976 nm with an average of 16.66 nm. The size of the nanoparticles is one of the important factors that govern the action of NPs. Its size is crucial for using NP in the drug delivery system as antiviral, antibacterial, and wound healing agents. Silver nano colloids in size range 3 nm–7 nm is an effective optimal dose for inhalation therapy for SARS-CoV-2 infection [23]. It is also reported that for effective antiviral action, the nanoparticles' size must be less than 10 nm. The geometrical limitation between glycoprotein protrusions in the form of spikes of coronaviruses or influenza viruses with the size of 100 nm and the NPs is if less, the NPs can effectively inhibit viral load. The size of the NPs and capping layer, and its composition influences the antiviral or antimicrobial action of NPs [24]. The high surface area and tiny particle size, NPs have been applied RT-PCR, ELISA, and RT-LAMP techniques to detect viral infection [3,25].

S. mutans is a well-known cariogenic bacterium causing dental caries in 60–80% of children and 100% adult population [26]. Before the dental caries formation, *S. mutans* makes a biofilm over the teeth; it metabolizes the fermentable carbohydrates into organic acids with low pH. The formed organic acids corrode the teeth' enamel leading to dental caries [27]. *S. mutans* is also found to cause endocarditis (Dafani, 1997). *S. mutans* are also reported to have developed multidrug resistance [28,29].

As *S. mutans* is exhibiting drug resistance, an alternate search with nanoparticles recommends GA-AgNPs as a good alternative. In the present study, GA-AgNPs were tested against *S. mutans*, causing dental caries in Fig. 6(a–c). The tested doses of GA-Ag NPs ranged between 25 μg/mL to 200 μg/mL. *S. mutans* growth was highly inhibited. The diameter of the zone of inhibition for 25 μg/mL, 50

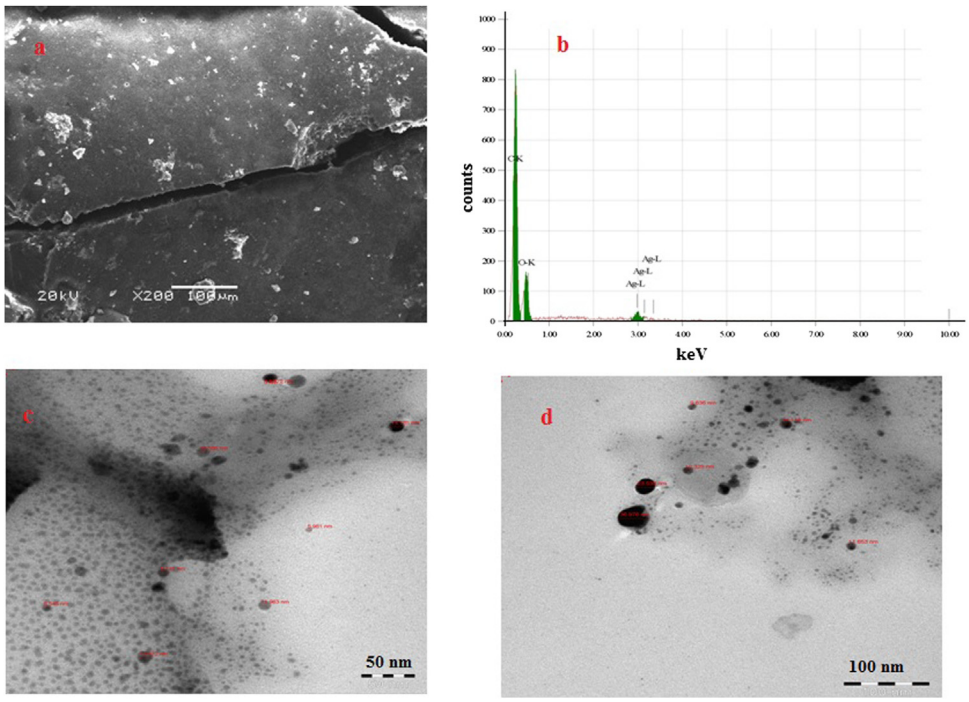

Fig. 5. Identification of shapes, size and elements using (a–b) TEM with different magnifications (c) SEM and (d) EADX of synthesized GA-AgNPs nanoparticles.

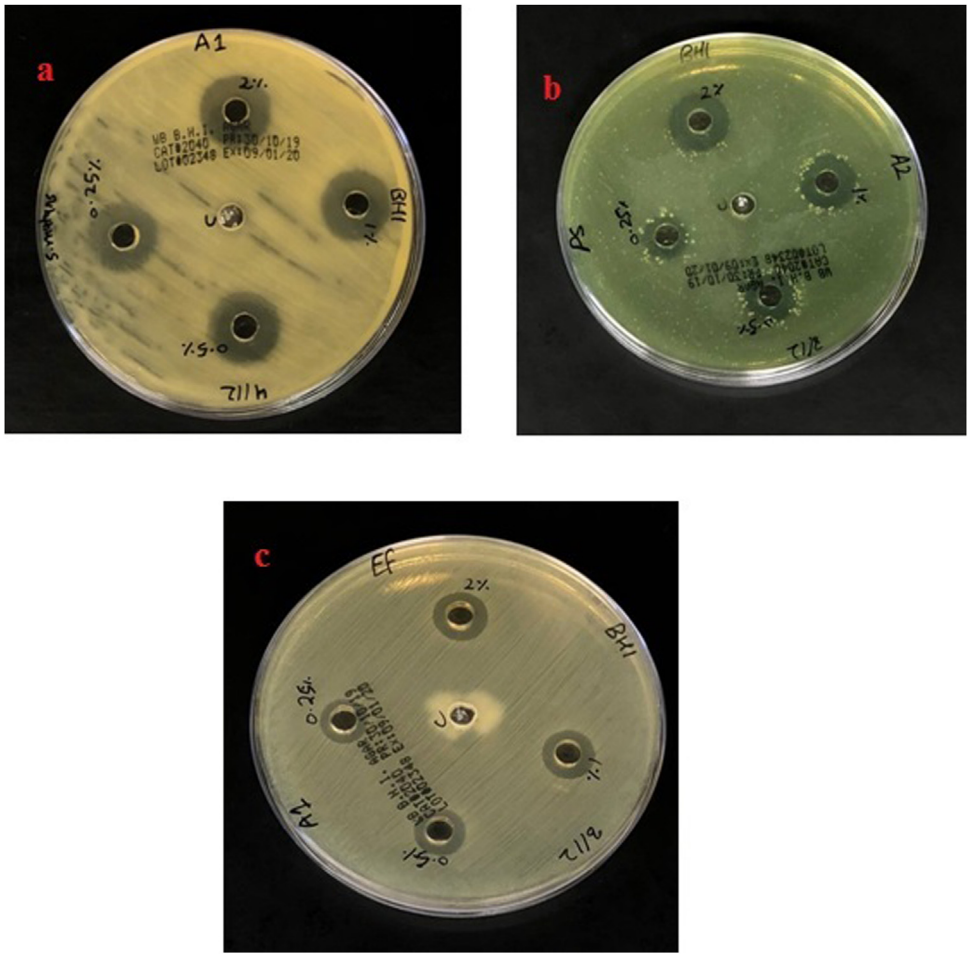

Fig. 6. Antibacterial effect of tested bacteria with GA-AgNPs with concentrations at (0.25%, 0.5%, 1%, 2%). (a) *S. mutans*; (b). *P. aeruginosa*; (c). *E. fecalis*.

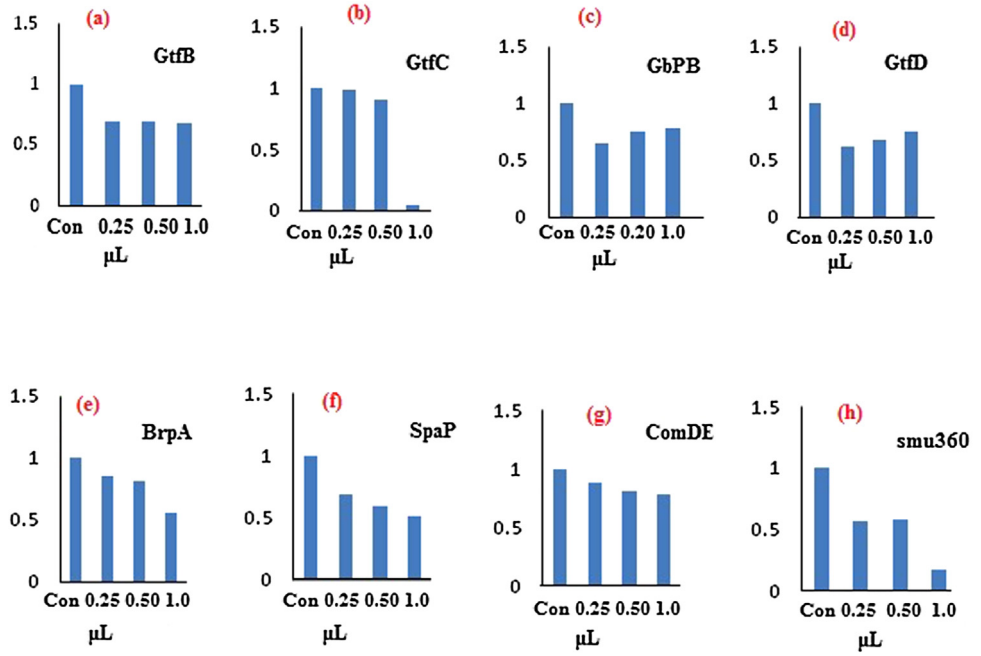

Fig. 7. Inhibition of virulence genes in *S. mutans* exposed to different concentrations of GA-AgNPs (a–h).

µg/mL, 100 µg/mL and 200 µg/mL were 14.05 ± 0.7, 15.5 ± 0.8, 16.3 ± 1.0 and 18.30 ± 0.5 nm respectively. The minimum inhibitory concentration of GA-AgNPs for *S. mutans* was 10.0 µg/mL. From the present study, it is evident that the synthesized AgNPs using gum Arabic can be used as an effective oral antibiotic to prevent dental caries by incorporating it with mouth wash and kinds of toothpaste. In *S. mutans* Glucosyl transference (gtfc gtfD and gtfB) are the virulent genes for plaque formation in biofilm over the tooth surface. The inhibition of the three glucosyltransferase genes impairs the colonization and biofilm formation by *S. mutans* [30]. The gene gtfD lies in a distant locus from gtfB, gtfC and gbpB (Fig. 7a–d). However, it plays a role in the structure of glucans in the biofilm formed by *S. mutans*. The inhibition of virulence of gftB, gftC and gftD interferes with the virulence of *S. mutans* and its biofilm formation over teeth that induces dental enamel corrosion and dental caries [30]. The glucan binding protein gbpB is another important virulent gene-regulating antibiotic sensitivity, oxidative and osmotic stress, cell wall construction, maintaining cell shape, hydrophobic, and biofilm formation [31]. A study showed that the mutation of gbpB gene in *S. mutans* altered the cell shape of *S. mutans*, leading to growth inhibition [32]. Fujita et al. reported that gbpB genes have several expression patterns according to the strain types of *S. mutans* [33]. The surface protein antigen 1/11 gene (spaP) is housekeeping genes in *S. mutans* interact with glycoprotein found in saliva to decide the receptors for the adhesion with teeth or gums, and its inhibition prevents *S. mutans* attachment with the teeth or gum of the host body [32].

The *S. mutans* (smu 360) gene studied in the present work is a hypothetical protein involved in establishing and surviving *S. mutans* in biofilm. The expression of smu 360 genes in *S. mutans* gets altered and inhibits biofilm formation under antibacterial blue light-induced oxidative stress [34]. The biofilm regulatory protein (brpA) of *S. mutans* plays a major role in the biofilm formation of *S. mutans*. The brpA gene is involved in systemic virulence in the blood [35]. Inhibition of brpA gene disturbs cell wall stress regulation, cohesiveness in biofilm and biofilm formation [36].

The gene regulation of treated *S. mutans* of *brpA*, spaP, comDE and smu 360 in Fig. 7e–h). The triple genes comDE, brpA and smu 360 are responsible for forming a protective extracellular matrix over *S. mutans* [37]. Any inhibition of these three genes prevents *S. mutans* colonization and growth. The competence regulation comDE gene is responsible for bacitracin production, cell formation, and competence [37,38]. So the inhibition of comDE by GA-AgNPs will paralyze the formation and survival of *S. mutans* in oral cavity. The gyra A gene studied is also an important virulent gene of *S. mutans*. The DNA gyrase encoding gyra A is a housekeeping gene offers protection to *S.mutans* against antibiotics and environmental stress [38,39]. In the present study, the synthesized GA-AgNPs inhibited the virulence of gyra Agene. From the evaluation of GA-AgNPs molecular inhibition of *S. mutans* showed that the different sets of genes, gtfB, gtfC, gtfD and gbpB responsible for biofilm formation, brpA, smu 360 and comDE responsible for protective extracellular matrix over *S. mutans* and spaP and gyrA genes for the survival of *S. mutans* in odd oral cavity ambiance are all inhibited [40]. The virulence gene expression study further strengthens the inhibitory action over the oral pathogen *S. mutans* causing dental caries and other diseases like endocarditis by GA-AgNPs by well diffusion assay.

Conclusion

The gum Arabica obtained from *Arabica senegal* is an ethnobotanical compound. The utilization of this natural medicinal product to tune silver nanoparticles' formation transferred its valuable components over the NPs as a capping and stabilizing agent. The gum Arabic moderated AgNPs are small in size with a maximum below 10 nm expands its application beyond the dental pathogen *S. mutans* to SARS-CoV-2 viral infection control. The COVID-19 viruses are reported to affect the upper respiratory tract as well as the oral cavity. So GA-AgNPs nasal spray or mouth wash can be used to eliminate the dental carcinogenic *S. mutans* and also other viruses causing respiratory-related problems.

Funding

King Saud University.

Competing interests

None declared.

Ethical approval

Not required.

Acknowledgement

The authors extend their appreciation to the Researchers Supporting Project number (RSP-2020/228), King Saud University, Riyadh, Saudi Arabia.

References

[1] Cavakcanti CDL, Nogueira MCBL. Pharmaceutical nanotechnology: which products are been designed against COVID-19? J Nanopart Res 2020;22:276.
[2] Weiss C, Carriere M, Fusco L, Capua I, Regla-Nava JA, et al. Toward nanotechnology-enabled approaches against the COVID-19 pandemic. ACS Nano 2020;14:6383–406.
[3] Medhi R, Srinoi P, Ngo N, Tran HV, Lee TR. Nanoparticle-based strategies to combat COVID-19. ACS Appl Nano Mater 2020;2020:0c01978.
[4] Yin XI, Zhao IS, Mei ML, Li Q, Yu OY, Chu CH. Use of silver nanomaterials for caries prevention: a concise review. Int J Nanomed 2020;15:3181–91.
[5] Adapa SB. A review on silver nanoparticles—the powerful nanoweapon against oral pathogens. Int J Oral Health Sci 2020;10:1–12.
[6] Lea R. Nanotechnology and the Fight against COVID-19. AZoNano; 2020 https://www.azonano.com/article.aspx?ArticleID=5540.
[7] Lea R. The Development of a New Anti-COVID-19 Nanocoating. AZoNano; 2020 https://www.azonano.com/news.aspx?newsID=37294.
[8] Chen L, Liang J. An overview of functional nanoparticles as novel emerging antiviral therapeutic agents. Mater Sci Eng C Mater Biol Appl 2020;112:110924.
[9] Campos EVR, Pereira AES, de Oliveira JL, Carvalho LB, Guilger-Casagrande M, de Lima R, et al. How can nanotechnology help to combat COVID-19? Opportunities and urgent need. J Nanobiotechnol 2020;18:125.
[10] Sarkar DS. Silver nanoparticles with bronchodilators through nebulisation to treat COVID 19 patients. J Curr Med Res Opin 2020;3:449–50.
[11] AlSalhi MS, Elangovan K, Ranjitsingh AJA, Murali P, Devanesan S. Synthesis of silver nanoparticles using plant derived 4-*N*-methyl benzoic acid and evaluation of antimicrobial, antioxidant and antitumor activity. Saudi J Biol Sci 2019;26:970–8.
[12] Devanesan S, AlSalhi MS, Balaji RV, Ranjitsingh AJA, Alfuraydi AA, AlQahtani FY, et al. Antimicrobial and cytotoxicity effects of synthesized silver nanoparticles from *Punica granatum* peel extract. Nanoscale Res Lett 2018;13:315.
[13] Al-Ansari MM, Dhasarathan P, Ranjitsingh AJA, Al-Humaid LA. *Ganoderma lucidum* inspired silver nanoparticles and its biomedical applications with special reference to drug resistant *Escherichia coli* isolates from CAUTI. Saudi J Biol Sci 2020;27:2993–3002.
[14] Alfuraydi AA, Devanesan S, Al-Ansari M, AlSalhi MS, Ranjitsingh AJ. Eco-friendly green synthesis of silver nanoparticles from the sesame oil cake and its potential anticancer and antimicrobial activities. J Photochem Photobiol B 2019;192:83–9.
[15] Garibo D, Borbón-Nuñez HA, de Leónm JND, García Mendoza E, et al. Green synthesis of silver nanoparticles using *Lysiloma acapulcensis* exhibit high-antimicrobial activity. Sci Rep 2020;10:12805.
[16] Bhavana V, Thakor P, Singh SB, Mehra NK. COVID-19: pathophysiology, treatment options, nanotechnology approaches, and research agenda to combating the SARS-CoV2 pandemic. Life Sci 2020;261:118336.
[17] Dwivedi LM, Shukla N, Baranwal K, Gupta S, Siddique S, Singh V. Gum Acacia modified Ni doped CuO nanoparticles: an excellent antibacterial material. J Clust Sci 2020, http://dx.doi.org/10.1007/s10876-020-01779-7.
[18] Kaddam L, Babiker R, Ali S, Satti S, Ali N, Elamin M, et al. Potential role of *Acacia senegal* (gum arabic) as immunomodulatory agent among newly diagnosed COVID 19 patients: a structured summary of a protocol for a randomised, controlled clinical trial. Trials 2020;21:766.
[19] Johnson W. Final report of the safety assessment of *Acacia catechu* gum, *Acacia concinna* fruit extract, *Acacia dealbata* leaf extract, *Acacia dealbata* leaf wax, *Acacia decurrens* extract, *Acacia farnesiana* extract, *Acacia farnesiana* flower wax, *Acacia farnesiana* gum. Int J Toxicol 2005;24:75–118.
[20] Al-Rafee MA, AlShammery AR, AlRumikan AS, Pani SC. A comparison of dental caries in urban and rural children of the Riyadh Region of Saudi Arabia. Front Public Health 2019;7:195.
[21] Li J, Wu T, Peng W, Zhu Y. Effects of resveratrol on cariogenic virulence properties of *Streptococcus mutans*. BMC Microbiol 2020;20:99.
[22] Velsankar K, Preethi R, Ram PJ, Ramesh M, Sudhahar S. Evaluations of biosynthesized Ag nanoparticles via *Allium sativum* flower extract in biological applications. Appl Nanosci 2020;10:3675–91.
[23] Pang B, Ma Y, Tian Z, Liu J, Wu S, Teng D, et al. Solvents-dependent selective fabrication of face-centered cubic and hexagonal close-packed structured ruthenium nanoparticles during liquid-phase laser ablation. J Colloid Interface Sci 2020:31349–97.
[24] John MS, Nagoth JA, Ramasamy KP, Mancini A, Giuli G, Natalello A, et al. Synthesis of bioactive silver nanoparticles by a *Pseudomonas* strain associated with the antarctic psychrophilic protozoon *Euplotes focardii*. Mar Drugs 2020;18:38.
[25] Rabiee N, Bagherzadeh M, Ghasemi A, Zare H, Ahmadi S, Fatahi Y, et al. Point-of-use rapid detection of SARS-CoV-2: nanotechnology-enabled solutions for the COVID-19 pandemic. Int J Mol Sci 2020;21:5126.
[26] Morris D, Ansar M, Speshock J, Ivanciuc T, Qu Y, Casola A, et al. Antiviral and immunomodulatory activity of silver nanoparticles in experimental RSV infection. Viruses 2019;11:732.
[27] Yang XX, Li C, Huang CZ. Curcumin modified silver nanoparticles for highly efficient inhibition of respiratory syncytial virus infection. Nanoscale 2016;8:3040–8.
[28] Al-Shami IZ, Al-Hamzi MA, Al-Shamahy HA, et al. Efficacy of some antibiotics against *Streptococcus mutans* associated with tooth decay in children and their mothers. J Dent Oral Health 2019;2:1–4.
[29] Murthy DPS, Channarayappa, Shanthakumar SS, Indiresha HN. Prevalence, characterization and heterogeneity studies on *Streptococcus mutans* isolated from Bangalore urban population. Int J Pharm Bio Sci 2014;5:122–8.
[30] Wang C, van der Mei HC, Busscher HJ, Ren R. *Streptococcus mutans* adhesion force sensing in multi-species oral biofilms. NPJ Biofilms Microbiomes 2020;6:25.
[31] Bowen WH, Koo H. Biology of *Streptococcus mutans*-derived glucosyltransferases: role in extracellular matrix formation of cariogenic biofilms. Caries Res 2011;45:69–86.
[32] Duque C, Stipp RN, Wang B, Smith DJ, Höfling JF, Kuramitsu HK, et al. Downregulation of GbpB, a component of the VicRK regulon, affects biofilm formation and cell surface characteristics of *Streptococcus mutans*. Infect Immun 2011;79:786–96.
[33] Fujita K, Takashima Y, Inagaki S, Nagayama K, Nomura R, Ardin AC, et al. Correlation of biological properties with glucan-binding protein B expression profile in *Streptococcus mutans* clinical isolates. Arch Oral Biol 2011;56:258–63.
[34] Klein MI, Xiao J, Lu B, Delahunty CM, Yates 3rd JR, Koo H. *Streptococcus mutans* protein synthesis during mixed-species biofilm development by high-throughput quantitative proteomics. PLoS One 2012;7:e45795.
[35] Nikinmaa S, Alapulli H, Auvinen P, Vaara M, Rantala J, Kankuri E, et al. Dual-light photodynamic therapy administered daily provides a sustained antibacterial effect on biofilm and prevents *Streptococcus mutans* adaptation. PLoS One 2020;15:e0232775.
[36] Wen ZT, Baker HV, Burne RA. Influence of BrpA on critical virulence attributes of *Streptococcus mutans*. J Bacteriol 2006;188:2983–92.
[37] Lemos JA, Palmer SR, Zeng L, Wen ZT, Kajfasz JK, Freires IA, et al. The biology of *Streptococcus mutans*. Microbiol Spectr 2019;7, http://dx.doi.org/10.1128/microbiolspec.GPP3-0051-2018.
[38] Loimaranta V, Mazurel D, Deng D, Söderling E. Xylitol and erythritol inhibit real-time biofilm formation of *Streptococcus mutans*. BMC Microbiol 2020;20:184.
[39] Xiong K, Chen X, Hu H, Hou H, Gao P, Zou L. Antimicrobial effect of a peptide containing novel oral spray on *Streptococcus mutans*. Biomed Res Int 2020;2020. ID 6853652.
[40] Shanmugam K, Sarveswari HB, Udayashankar A, Swamy SS, Pudipeddi A, Shanmugam T, et al. Guardian genes ensuring subsistence of oral *Streptococcus mutans*. Crit Rev Microbiol 2020;46, 475–49.